Two-Dimensional Confinement of $3d^1$ Electrons in $LaTiO_3/LaAlO_3$ Multilayers

S. S. A. Seo,[1,2,*] M. J. Han,[1,†] G. W. J. Hassink,[3,4] W. S. Choi,[1] S. J. Moon,[1] J. S. Kim,[2,‡] T. Susaki,[3] Y. S. Lee,[5] J. Yu,[1] C. Bernhard,[6] H. Y. Hwang,[3,7] G. Rijnders,[4] D. H. A. Blank,[4] B. Keimer,[2] and T. W. Noh[1,§]

[1]*Department of Physics and Astronomy, Seoul National University, Seoul 151-747, Korea*
[2]*Max-Planck-Institut für Festkörperforschung, Stuttgart D-70569, Germany*
[3]*Department of Advanced Materials Science, University of Tokyo, Kashiwa, Chiba 277-8561, Japan*
[4]*MESA+ Institute for Nanotechnology, University of Twente, Enschede NL-7500 AE, The Netherlands*
[5]*Department of Physics, Soongsil University, Seoul 156-743, Korea*
[6]*Department of Physics and Fribourg Center for Nanomaterials, University of Fribourg, 1700 Fribourg, Switzerland*
[7]*Japan Science and Technology Agency, Kawaguchi 332-0012, Japan*

(Received 23 October 2009; published 19 January 2010)

We report spectroscopic ellipsometry measurements of the anisotropy of the interband transitions parallel and perpendicular to the planes of $(LaTiO_3)n(LaAlO_3)5$ multilayers with $n = 1$–3. These provide direct information about the electronic structure of the two-dimensional (2D) $3d^1$ state of the Ti ions. In combination with local density approximation, including a Hubbard U calculation, we suggest that 2D confinement in the TiO_2 slabs lifts the degeneracy of the t_{2g} states leaving only the planar d_{xy} orbitals occupied. We outline that these multilayers can serve as a model system for the study of the t_{2g} 2D Hubbard model.

DOI: 10.1103/PhysRevLett.104.036401 PACS numbers: 71.27.+a, 73.21.Ac, 78.67.De, 78.67.Pt

Recent advances of oxide thin-film synthesis techniques enable the study of oxide multilayers with atomically abrupt interfaces [1,2]. Pioneering studies on various oxide heterostructures have revealed intriguing physical phenomena such as electronic reconstruction [3,4], quantum Hall effect [5], and orbital reconstruction [6] at the interfaces. A new approach of dimensionality control of oxides has also been made possible by the potential well (or quantum well) geometry of $LaMO_3/LaAlO_3$ (M: transition metal elements) since the Al $3p$ state is located much higher in energy than the transition metal $3d$ state [7]. Recent theoretical studies have brought particular attention to the potential well geometry since intriguing physical properties can be manipulated in such multilayered structures. For instance, high-T_c superconductivity was predicted to occur in $LaNiO_3/LaAlO_3$ [8].

In this Letter, we report the electronic structure and orbital reconstruction of $3d^1$ electrons in multilayers consisting of a few unit-cell $LaTiO_3$ (LTO) layers embedded in $LaAlO_3$ (LAO) using optical spectroscopic ellipsometry and LDA + U calculations (LDA: local density approximation). Single crystalline LTO is a Mott insulator with a small Mott-Hubbard gap of ~0.2 eV [9] while LAO is a band insulator with a wide band gap of ~5.6 eV. By taking into account the electronic structures of the bulk phases, a two-dimensional (2D) confinement of the Ti $3d^1$ state in LTO/LAO multilayers can be considered [Fig. 1(a)] similarly to the V $3d^2$ state in $LaVO_3$/LAO of Ref. [7]. This 2D Ti^{3+} state is particularly interesting since a bulk material possessing a $Ti^{3+}O_2$ 2D square lattice has not yet been found. In analyzing the interband optical transitions, we show that a 2D confined $3d^1$ Mott state can be realized in the LTO/LAO multilayers. Along with the confinement, the Ti $3d$ orbitals are also reconstructed, as the threefold degeneracy of the t_{2g} levels is lifted yielding partially occupied d_{xy} and empty $d_{yz,zx}$ orbitals.

By using the pulsed laser deposition technique, we grew multilayers of $[(LTO)n(LAO)5] \times 20$, which means 20 repetitions of n (=1, 2, and 3) pseudocubic perovskite unit cell(s) of LTO (~$n \times 3.96$ Å) and five pseudocubic unit-cells of LAO (~5×3.78 Å), on $SrTiO_3$ (STO) (001) substrates. (Details about the growth can be found in the supplementary online material [10].) The relevant parameter concerning quantum confinement is the ratio of the potential well width of the multilayers and the excitonic

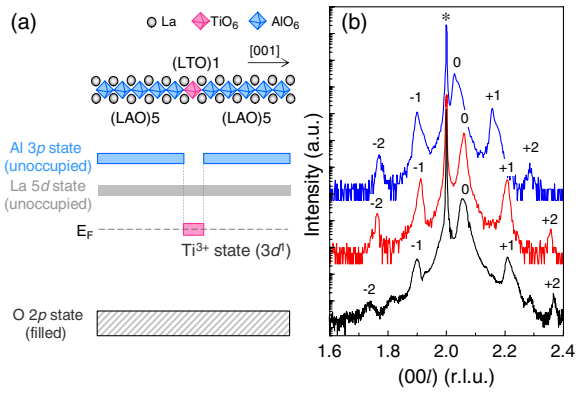

FIG. 1 (color online). (a) Schematic of the energy levels of a multilayer of (LTO)1(LAO)5, showing a potential well geometry. (b) X-ray Bragg reflections around the STO 002 (*), and superlattice satellite peaks of the (LTO)3(LAO)5, (LTO)2(LAO)5, and (LTO)1(LAO)5 multilayers (from top to bottom).

radius $a_0 = a_B\varepsilon/m^*$ [11], where $a_B(= 0.53$ Å) is the hydrogenic Bohr radius, ε is the dielectric permittivity, and m^* is the effective electronic mass in LTO. With reasonable estimates of $m^* \approx 2$–4 and $\varepsilon \approx 20$–50, we obtain $a_0 \approx 3$–13 Å. Hence, in this study we pursued LTO layers with $n < 4$.

Figure 1(b) shows x-ray θ-2θ scans around the STO 002 reflection, which reveal sharp superlattice satellite peaks due to the periodicity of the multilayer. The Δl between the satellite peaks satisfies the relation $\Delta l = 1/(n + 5)$ in each (LTO)n(LAO)5 multilayer. X-ray reciprocal space mappings confirmed that the averaged in-plane lattice constants were coherently strained to those of the STO substrates. Although a nonstoichiometric phase with excessive oxygen $LaTiO_{3+\delta}$ [12] or La vacancies $La_{1-x}TiO_3$ [13] is known to be metallic, our multilayers were highly insulating in the measurements of dc conductivity and optical absorption spectroscopy [14].

To investigate the electronic structure of the (LTO)n(LAO)5 multilayers, we used bulk-sensitive spectroscopic ellipsometry in the ultraviolet photon energy region, i.e., 3.3–6.5 eV, which is compatible with the energies of interband optical transitions of LTO. Spectroscopic ellipsometry is a self-normalizing technique that directly measures the complex dielectric function $\tilde{\varepsilon}(\omega)[= \varepsilon_1(\omega) + i\varepsilon_2(\omega)]$ of a multilayer without the need of Kramers-Kronig transformation. (See the supplementary material for details on the spectroscopic ellipsometry measurements and analyses [10].) Since the probing depth of this technique is typically longer than about 500 Å, it is very useful to characterize buried interfaces and layers. Ellipsometry is also advantageous in determining the in-plane and out-of-plane optical responses of anisotropic materials.

Figure 2 shows the anisotropy of the optical conductivity spectra $[\sigma_1(\omega)]$ of the (LTO)n(LAO)5 ($n = 1$, 2, and 3) multilayers. They were obtained by using the relation of $\tilde{\varepsilon}(\omega) = \varepsilon_1(\omega) + i4\pi\sigma_1(\omega)/\omega$. The parameters characterizing the optical transitions were obtained by fitting to Lorentz oscillators:

$$\tilde{\varepsilon}(\omega) = \epsilon_\infty + \sum_j \frac{S_{0j}\omega_{0j}^2}{\omega_{0j}^2 - \omega^2 - i\omega\Gamma}. \quad (1)$$

The results of this fit procedure are shown by the solid lines. (The values of the fitting parameters are listed in Table 1 of the supplementary material [10].) There are two broad peaks in the in-plane ($E \parallel ab$) optical spectra. The low energy peak (α) and the high energy peak (β) can be assigned as charge transfer transitions from the O $2p$ state to the unoccupied Ti $3d$ t_{2g} and to the Ti $3d$ e_g states, respectively. The energy difference between the two optical transitions gives the crystal field splitting, $10Dq$ of the Ti $3d$ state [15]. It is noteworthy that the α-peak position increases as the thickness of LTO layers decreases while the β-peak position remains almost unchanged. The inset

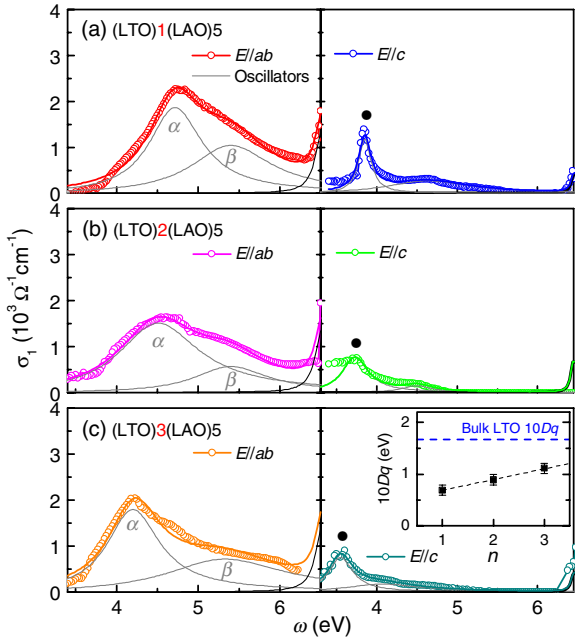

FIG. 2 (color online). In-plane (left) and out-of-plane (right) components of the optical conductivity spectra of the (LTO)n(LAO)5 multilayers with (a) $n = 1$, (b) $n = 2$, and (c) $n = 3$. [Inset of (c)] $10Dq$ of Ti^{3+} as a function of n. The dashed (blue) line gives the value in bulk LTO [17].

of Fig. 2(c) shows how $10Dq$ of the Ti $3d$ levels depends on the LTO sublayer thickness in comparison to the value of 1.67 eV [17] in bulk LTO.

Another notable feature is a sharp peak (•) around 3.7 eV in the out-of-plane ($E \parallel c$) spectra, which has not been observed in any bulk crystals nor thin films of LTO and LAO. In general, an interband optical transition intensity $I_{i\to f}$ from an initial state i to a final state f at $\hbar\omega_0$ can be described as $I_{i\to f}(\hbar\omega_0) = \int |\langle f|M|i\rangle|^2 \rho_f(\omega)\rho_i(\omega - \hbar\omega_0)d\omega$ according to the Fermi golden rule, where M is the matrix element, and ρ_i and ρ_f are the densities of states for i and f, respectively. Hence, a sharp optical conductivity peak usually appears when it involves both narrow-bandwidth initial (occupied) and final (unoccupied) states such as quantized levels in a quantum well. Since the Ti-O hybridization becomes weaker along the out-of-plane direction than that along the in-plane directions, a narrowing of the bonding state and a reduced bonding-antibonding separation are expected. Although the origin of the peak around 3.7 eV still remains unclear at this moment, it may be a signature of the asymmetric hybridization in the layered structure, which causes major modifications of the electronic structure and optical properties. Note that all of these experimental spectra cannot be explained by the 2D effective medium approximation [18] using the spectra of bulk LTO (Ref. [19]) and LAO (Ref. [16]). This also suggests that the electronic structure of these multilayers is not a simple average of the two mother compounds but rather strongly reconstructed.

To examine more details of the electronic structure and magnetic properties, we performed LDA + U calculations with the on-site Coulomb energy U ($\equiv \tilde{U} - J = 6$ eV) [10,20], which is consistent with previous studies on bulk LTO [21,22]. The magnetic ground state is a checkerboard type antiferromagnetic (AFM) spin order which is more stable than the striped AFM and ferromagnetic ordering. It is noteworthy that the spin structure is similar to that of the undoped cuprates. Figure 3 shows the spin-averaged partial density of states (PDOS) of the TiO_2 slabs in the (LTO)n(LAO)5 multilayers. One of the most remarkable points is that the threefold degeneracy in the t_{2g} state is lifted and the d_{xy} orbital is partially occupied while $d_{yz,zx}$ states are pushed to higher energies. On the other hand, the isotropic spin wave spectrum observed below the Néel temperature ($T_N = 140$–150 K) of bulk LTO has suggested strong orbital fluctuations [23]. Such a disordered orbital state in a cubic lattice is very unusual, and similar disorder occurs when mobile carriers are present in e_g orbital systems such as the manganites [24]. Moreover, ferromagnetic ordering is more favored than AFM ordering when t_{2g} orbitals are degenerate in the cubic lattice [25]. The theoretical description of the orbital state of bulk LTO is still under debate (see, e.g., Refs. [26]). However, in the 2D (LTO)n(LAO)5 multilayers, the orbital degeneracy can be easily lifted, and a d_{xy}-orbital configuration, which is different from that of 3D bulk LTO, can be formed. This notable difference of the electronic structure from that of the bulk counterpart is most likely caused by the heterointerfaces. Because of the existence of the LAO layers, the hybridization of Ti-3d levels with O-2p becomes asymmetric: the d_{xy} states hybridize two dimensionally with the in-plane oxygens while the hybridization between $d_{yz,zx}$ states and out-of-plane oxygens is weaker. A similar planar orbital reconstruction has also been suggested for LTO-STO 2D superlattices [27].

The lifted degeneracy of the t_{2g} state and the d_{xy}-orbital occupation in the (LTO)n(LAO)5 multilayer is indeed consistent with the optical spectra. We estimate that the gap energy between the d_{xy} orbital and $d_{yz,zx}$ states increases by about 0.6 eV as n decreases from $n = 3$ to $n = 1$ (Fig. 3). Since the Ti e_g states remain at the same energy, the value of $10Dq$ decreases as n decreases. Such a change of $10Dq$ might be induced by a local lattice distortion, i.e., a change of the Ti-O-Ti bond angle and/or distance, which is proportional to $d_r^{1.5}/d_{\mathrm{Ti\text{-}O}}^{3.5}$ [28], where d_r is the radial size of the d orbital and $d_{\mathrm{Ti\text{-}O}}$ is the distance between Ti and O ions. However, in our multilayer samples, the in-plane lattice constants are fully strained to the STO substrates such that the lateral Ti-O distance does not change very much. We might still have to consider stronger lattice distortions around TiO_6 octahedra by local strains for the thinner LTO layers, but the experimentally observed $10Dq$ values do not increase but decrease as n decreases [Fig. 2(c) inset]. Hence, lattice distortions cannot be a reason for the electronic changes. Based on our optical

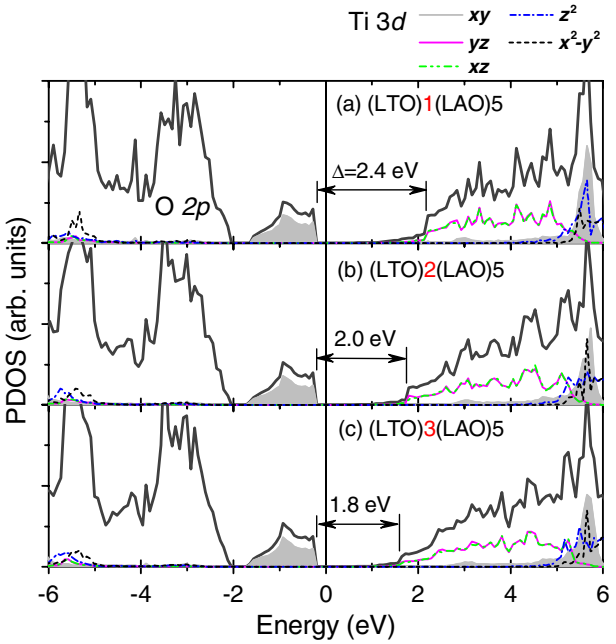

FIG. 3 (color online). The partial density of states of the TiO_2 slabs in (a) (LTO)1(LAO)5, (b) (LTO)2(LAO)5, and (c) (LTO)3(LAO)5 multilayers calculated by LDA + U. Δ indicates the energy gap between the occupied d_{xy} orbital and the unoccupied $d_{yz,zx}$ states.

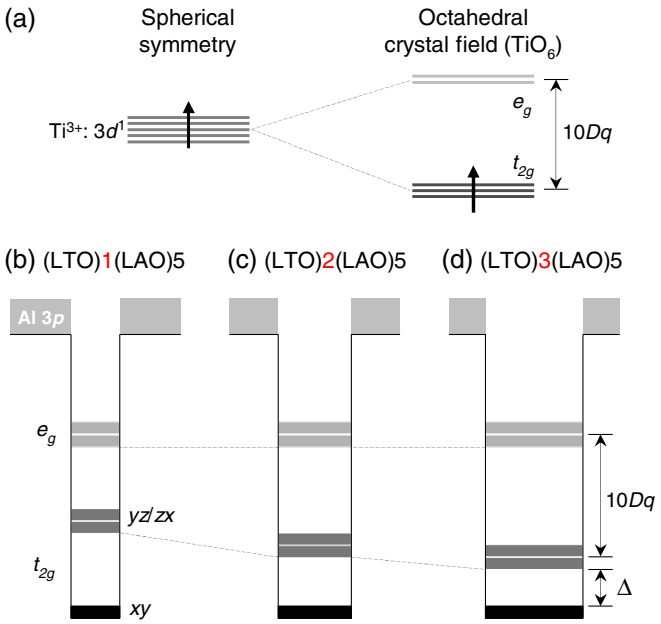

FIG. 4 (color online). (a) Crystal field splitting of a Ti 3d state in octahedral symmetry. Schematic diagram of additional energy splitting (Δ) of the t_{2g} state in the multilayers of (b) (LTO)1(LAO)5, (c) (LTO)2(LAO), and (d) (LTO)3(LAO)5 due to the 2D confinement.

spectroscopic results and LDA + U calculations, Ti $3d$ energies in the (LTO)n(LAO)5 multilayer potential wells can be schematically summarized as in Figs. 4(b)–4(d). We believe that the electronic 2D confinement in the TiO_2 plane plays the most important role in the stabilization of the planar d_{xy}-orbital configuration.

In conclusion, our experimental and theoretical results suggest that the Ti $3d^1$ states have a ferro-orbital configuration with only d_{xy}-orbital occupation in the 2D TiO_2 slabs. As we narrow the thickness of the confined TiO_2 slabs to a monolayer, the d_{xy} orbitals become more stable due to the larger energy gap between the states of d_{xy} and $d_{yz,zx}$ in a t_{2g} level. The 2D confinement of a single electron in a Ti $3d_{xy}$ level results in an electronic structure that is isomorphic to that of the undoped precursors of the cuprate high-T_c superconductors. It should therefore be interesting to systematically vary the layer thickness, layer sequence, and doping level of these structures.

S. S. A. S. thanks A. Fujimori, G. Jackeli, G. Khaliullin, S. Okamoto, and A. V. Boris for useful discussions. M. J. H. is indebted to A. J. Millis and C. A. Marianetti for valuable insights. This research was supported by the Basic Science Research Program through the National Research Foundation of Korea funded by the Ministry of Education, Science, and Technology (No. 2009-0080567 and No. R17-2008-033-01000-0), a nanotechnology program of the Dutch Ministry of Economic Affairs (NanoNed), the Swiss National Science Foundation (SNF Project No. 20020-119784), and the German Science Foundation (SFB/TRR 80).

*Current address: Materials Science and Technology Division, Oak Ridge National Laboratory, Oak Ridge, TN 37831, USA.
seos@ornl.gov

†Current address: Department of Physics, Columbia University, New York, NY 10027, USA.

‡Current address: Department of Physics, Pohang University of Science and Technology, Pohang, Kyungbuk 790-784, Korea.

§twnoh@snu.ac.kr

[1] A. Ohtomo *et al.*, Nature (London) **419**, 378 (2002).
[2] H. N. Lee *et al.*, Nature (London) **433**, 395 (2005).
[3] S. Okamoto and A. J. Millis, Nature (London) **428**, 630 (2004).
[4] S. S. A. Seo *et al.*, Phys. Rev. Lett. **99**, 266801 (2007).
[5] A. Tsukazaki *et al.*, Science **315**, 1388 (2007).
[6] J. Chakhalian *et al.*, Science **318**, 1114 (2007).
[7] Y. Hotta *et al.*, Appl. Phys. Lett. **89**, 251916 (2006); H. Wadati *et al.*, Phys. Rev. B **77**, 045122 (2008); T. Higuchi, Y. Hotta, T. Susaki, A. Fujimori, and H. Y. Hwang, Phys. Rev. B **79**, 075415 (2009); M. Takizawa *et al.*, Phys. Rev. Lett. **102**, 236401 (2009).
[8] J. Chaloupka and G. Khaliullin, Phys. Rev. Lett. **100**, 016404 (2008); P. Hansmann *et al.*, Phys. Rev. Lett. **103**, 016401 (2009).
[9] Y. Okimoto, T. Katsufuji, Y. Okada, T. Arima, and Y. Tokura, Phys. Rev. B **51**, 9581 (1995).
[10] See supplementary material at http://link.aps.org/supplemental/10.1103/PhysRevLett.104.036401.
[11] P. A. Cox, *Transition Metal Oxides: An Introduction to Their Electronic Structure and Properties* (Oxford University Press, New York, 1992).
[12] A. Schmehl *et al.*, Appl. Phys. Lett. **82**, 3077 (2003).
[13] D. A. Crandles, T. Timusk, J. D. Garrett, and J. E. Greedan, Phys. Rev. B **49**, 16 207 (1994).
[14] S. S. A. Seo *et al.*, Appl. Phys. Lett. **95**, 082107 (2009).
[15] Another charge transfer transition from O $2p$ to La $5d$ would be located above 5.6 eV (Ref. [16]), which is beyond our measurement range.
[16] S.-G. Lim *et al.*, J. Appl. Phys. **91**, 4500 (2002).
[17] T. Higuchi *et al.*, Phys. Rev. B **68**, 104420 (2003).
[18] V. M. Agranovich and V. E. Kravtsov, Solid State Commun. **55**, 85 (1985).
[19] T. Arima and Y. Tokura, J. Phys. Soc. Jpn. **64**, 2488 (1995).
[20] M. J. Han, T. Ozaki, and J. Yu, Phys. Rev. B **73**, 045110 (2006); M. J. Han and J. Yu, J. Korean Phys. Soc. **53**, 1074 (2008).
[21] I. Solovyev, N. Hamada, and K. Terakura, Phys. Rev. B **53**, 7158 (1996).
[22] E. Pavarini *et al.*, Phys. Rev. Lett. **92**, 176403 (2004).
[23] B. Keimer *et al.*, Phys. Rev. Lett. **85**, 3946 (2000).
[24] S. Ishihara, M. Yamanaka, and N. Nagaosa, Phys. Rev. B **56**, 686 (1997).
[25] S. Ishihara, T. Hatakeyama, and S. Maekawa, Phys. Rev. B **65**, 064442 (2002).
[26] G. Khaliullin and S. Maekawa, Phys. Rev. Lett. **85**, 3950 (2000); M. Mochizuki and M. Imada, Phys. Rev. Lett. **91**, 167203 (2003); M. W. Haverkort *et al.*, Phys. Rev. Lett. **94**, 056401 (2005).
[27] R. Pentcheva and W. E. Pickett, Phys. Rev. Lett. **99**, 016802 (2007).
[28] W. A. Harrison, *Electronic Structure and Physical Properties of Solids* (Freeman, San Francisco, 1980).